

MODELLING OF FUNDAMENTAL PROPERTIES OF CARBON NANOTUBES

Yury Shunin, Victor Gopeyenko

*Information Systems Management Institute
Department of Natural Sciences and Computer Technologies
E-mail: shunin@isma.lv, Viktors.Gopeyenko@isma.lv*

The scattering theory approach gives possibilities to calculate an electronic structure and elastic properties of condensed media, which should be considered as static phenomena. At the same time this approach is convenient for the electron transport modelling, which is a dynamical problem. It is the principal distinctive feature as compared to a tight-binding theory, where transport phenomena defy description. Some special problems of multiple scattering theory approach for effective media electronic structure calculations of carbon nanotubes, which are considered as perspective elements of nanodevices for computer technologies are studied.

Keywords: multiple scattering theory, carbon nanotubes

1. Introduction

The electrical resistance of contacts between the carbon nanotubes (CNT) and the nickel catalytic substrate can considerably exceed that observed in separate parts of these interconnects [1, 2]. Conductance between real metals and CNT still occurs, however, mainly due to scattering processes which are estimated rather weak [3]. Fig. 1 depicts the idealized image of contacts between the CNTs and Ni substrate. The toroidal region (C-Ni) is the object of microscopic approach responsible for the main contribution into resistance. As to the nanotube itself and metallic substrate, their resistances may be considered as the macroscopic parameters. The electronic structure for the CNT-Ni interconnecting can be evaluated through the electronic density of states (DOS) for C-Ni contact considered as ‘disordered alloy’, where clusters containing both C and Ni atoms are the centres of scattering (Section 1). Computational procedure developed by us for these calculations [4] is based on construction of the cluster potentials and evaluation of the S - and T -matrices of scattering and transfer, respectively (Fig. 2 [5]). The cluster formalism was successfully implemented for metallic Cu [4] as well as for both elemental (Ge and Si) and binary (As-, Sb-, and Se-containing) semiconductors [6, 7]. Special attention was paid to the latter since As_xSe_{1-x} and Sb_xSe_{1-x} are not only prospective materials for the optical recording [7] but the concept of statistical weighing was applied here for the binary components. Using the coherent potential approach (CPA) as an effective-medium-approximation (EMA) the resistance of interconnecting can be evaluated through the Kubo-Greenwood formalism [8] and Ziman model [9].

Simultaneously, we perform the first principles DFT-LCAO calculations (as implemented in *CRYSTAL* code [10]) on the periodic 2D models of short (~0.85 nm height) single-walled CNTs of certain chirality’s with uniform ~1 nm diameter periodically contacted to the infinite three-layer Ni(111) surface (Section 2) which possesses a minimal surface energy among the densely packed nickel substrates. Methodology of *CRYSTAL* calculations on both perfect and defective nanotubes was recently developed by us for AlN NTs [11,12] whereas for metal surface reactivity, it was applied when describing the aluminum oxidation mechanism through the interaction of the densely packed Al surfaces with the molecular and atomic oxygen [13].

2. Effective Media Electronic Structure Calculations of CNT-Ni Interconnects

The scattering theory approach gives possibilities to calculate an electronic structure and elastic properties of condensed media, which should be considered as static phenomena. At the same time this approach is convenient for the electron transport modeling, which is a dynamical problem. It is the principal distinctive

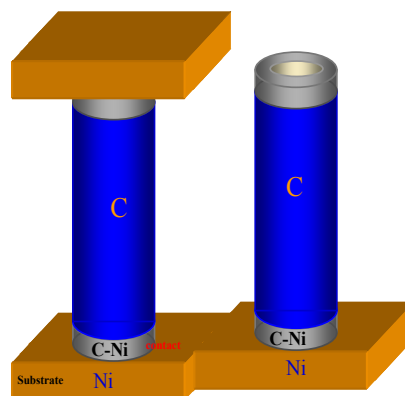


Figure 1. Fragment of interconnects between the Ni substrate and C nanotubes

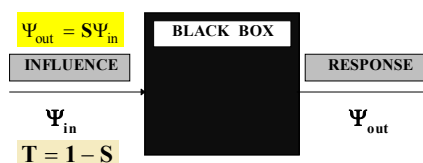


Figure 2. Scattering principle

feature as compared to a tight-binding theory, where transport phenomena defy description. Meanwhile, the scattering theory approach (when using quasi-free electron formalism) is also not free of shortcomings. Certain simplifications are necessary to obtain reliable results [4-7], for example, the CPA considered as an effective-medium-approximation.

2.1. Potential constructions: atomic and crystalline

An electronic structure calculation is considered here as a scattering problem, where centers of scattering are atoms of clusters. The first step of modeling is the construction of potentials, both atomic and crystalline. The Gaspar's potential of screened atomic nucleus looks as follows:

$$V^G(\mathbf{r}) = -\frac{2Z \exp(-\lambda r / \mu)}{r(1 + Ar / \mu)}, \quad (2.1.1)$$

where $\lambda = 0,1837$, $\mu = 0,8853Z^{-1/3}$, $A = 1,05$. Therefore, $V_e^G(\mathbf{r}) = 2Z/r - V^G(\mathbf{r})$ is the electronic part of Gaspar's potential. Using a statistical approach of atoms, one usually applied X_α and $X_{\alpha\beta}$ presentations for the electronic exchange and correlation:

$$V_{X_\alpha}(\mathbf{r}) = -6\alpha(3\rho/8\pi)^{1/3}, \quad (2.1.2)$$

$$V_{X_{\alpha\beta}}(\mathbf{r}) = \left[1 + \frac{\beta}{\alpha}G(\rho)\right]V_{X_\alpha}, \quad (2.1.3)$$

where $G(\rho) = \frac{4}{3}\left(\frac{\nabla\rho}{\rho}\right)^2 - 2\frac{\nabla^2\rho}{\rho}$, $\alpha = 0,67$ (α depends on the charge number Z), $\beta = 0,003$, and

$\rho(\mathbf{r}) = \nabla_r V_e^G(\mathbf{r})/8\pi$ (function of the electronic density). Thus, the atomic potential of a neutral atom can be expressed as:

$$V_{at}(\mathbf{r}) = V_{Coul}(\mathbf{r}) + V_{ex-corr}(\mathbf{r}), \quad (2.1.4)$$

where we consider V_{Coul} as Gaspar's potential and $V_{ex-corr}$ as potentials V_{X_α} or $V_{X_{\alpha\beta}}$.

The crystalline potential and electronic density can be expressed by formulae:

$$V_{Coul}(\mathbf{r}) = V^G(\mathbf{r}) + \sum_{\gamma, n_\gamma} V_\gamma^G(\mathbf{r} - \mathbf{R}_n^\gamma), \quad (2.1.5)$$

$$\rho_{cryst}(\mathbf{r}) = \rho(\mathbf{r}) + \sum_{\gamma, n_\gamma} \rho_\gamma(\mathbf{r} - \mathbf{R}_n^\gamma), \quad (2.1.6)$$

where γ defines summing up over the crystalline unit cells and \mathbf{R}_n^γ are the interatomic distances. (Fig. 3 shows both atomic and crystalline potentials for carbon in comparison with Hartree-Fock atomic potential). Then, we apply the so-called muffin tin approximation (*MTA*):

$$V_{MT}(\mathbf{r}) = \langle V_{cryst}(\mathbf{r}) \rangle - V_{MTZ}, \quad (2.1.7)$$

$$V_{cryst}(\mathbf{r}) = V_{Coul}(\mathbf{r}) + V_{ex-corr}(\mathbf{r}), \quad (2.1.8)$$

where $V_{ex-corr}$ are the same potentials V_{X_α} or $V_{X_{\alpha\beta}}$ as in atomic case except for the electronic density, which is defined according to Eq. (2.1.6), V_{MTZ} the *MT*-zero estimate of potential calculation. To obtain the electronic structure, the calculation of scattering properties is necessary, generally, in the form of *S*- and *T*-matrices (Fig. 2). An important case of *MT*-potentials has been widely studied, but much attention was paid to the spherical non-symmetrical potentials. The results of potential modelling and phase shifts in the framework of the *MT*-approximation are presented in Refs. [6, 7].

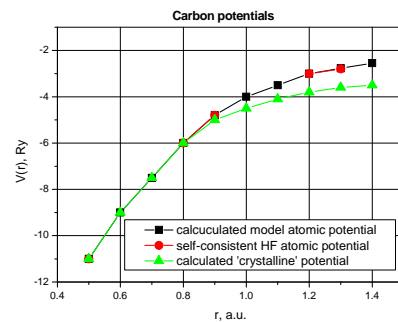


Figure 3. Analytical C potentials compared with results of HF calculations

2.2. Electronic structure and conductivity

The electronic structure calculations start from the definition of the initial atomic structure to produce a medium for solution of the scattering problem for a trial electronic wave (see Fig. 4) [5-7]. The formalism we use for electronic structure calculations is based on the CPA, the multiple scattering theory and cluster approach. As the first step in the modelling procedure, one postulates the atomic structure on the level of short- and medium-range orders.

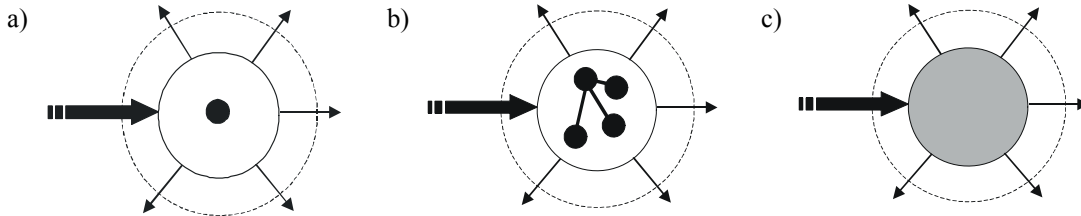


Figure 4. Models of the scattering clusters: a) single atom cluster; b) many-atomic cluster; c) cluster with the general type potential in an effective medium, with the dispersion relation $E(\mathbf{k})$ and a complex energy-dependent coherent potential $\Sigma(E)$, which is found self-consistently in the framework of the CPA

The next step is to construct a "crystalline" potential and introduce the *MTA*. This is accomplished by using realistic analytical potential functions. Then, the electronic wave scattering problem is solved, and the energy dependence of the scattering properties for isolated muffin-tin scatterers is obtained in the form of *phase shifts* $\delta_{lm}(E)$ (see Fig. 5), and the *T*-matrix of the cluster as a whole is found. The indices l and m arise as a result of expansions of the functions as Bessel's functions j_l , Hankel's functions h_l and spherical harmonics Y_{lm} . We note that the introduction for the potentials simplifies the solution of the scattering problem considerably since this procedure symmetrizes the potentials. In this case, the scattering is defined by radial component R_l only. However, the analysis of the scattering problem for potential functions of a general type not possessing spherical symmetry within the confines of the cluster volume has demonstrated that the *MTA* is applicable for a wide class of disordered materials, both metals and semiconductors. In the procedure of constructing the potentials, the $X_{\alpha\beta}$ approximation for the exchange-correlation interaction has also been used. This approximation has important advantages for describing binary materials since its α and β parameters are practically constant for different elements.

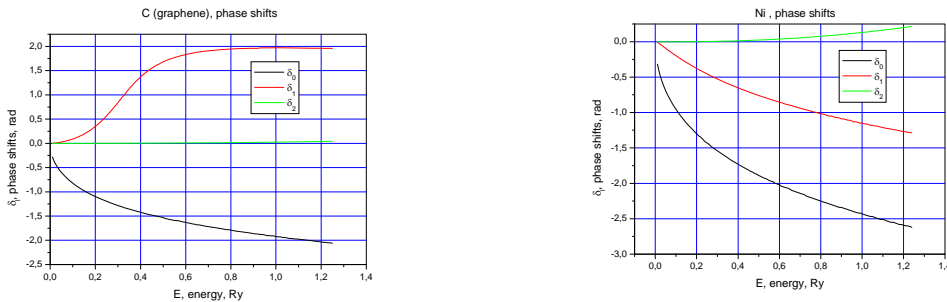


Figure 5. Phase shifts for graphene (C) and nickel (Ni) atomic clusters

The modelling of disordered materials represent them as a set of atoms or clusters immersed in an effective medium with the dispersion $E(\mathbf{k})$ and a complex energy-dependent coherent potential $\Sigma(E)$ found self-consistently in the framework of the CPA. The basic equations of this approach are:

$$\Sigma(E) = V_e + \langle T \rangle (1 + G_e \langle T \rangle)^{-1}, \quad (2.2.1)$$

$$G(E) = G_e + G_e \langle T \rangle G_e = \langle G \rangle, \quad (2.2.2)$$

$$\langle T(E, \mathbf{k}) \rangle = 0, \quad (2.2.3)$$

$$\Sigma(E) = V_e, \quad (2.2.4)$$

$$\langle G \rangle = G(E) = G_e, \quad (2.2.5)$$

$$N(E) = -(2/\pi) \ln \{ \det \| G(E) \| \} . \quad (2.2.6)$$

Here $\langle \dots \rangle$ denotes configurational averaging, V and G are the potential and the Green's function of the effective medium, respectively (see Subsection 1.3), $T(E, \mathbf{k})$ the T matrix of the cluster, and $N(E)$ the integral density of the electronic states. Eq. (2.2.3) can be re-written in form:

$$\langle T(E, \mathbf{k}) \rangle = \mathbf{Sp} T(E, \mathbf{k}) = \int \langle \mathbf{k} | T(E, \mathbf{k}) | \mathbf{k} \rangle d\Omega_{\mathbf{k}} = 0 , \quad (2.2.7)$$

where $|\mathbf{k}\rangle = 4\pi \sum_{l,m} (\mathbf{k}\mathbf{r})^l j_l(\mathbf{k}\mathbf{r}) Y_{lm}^*(\mathbf{k}) Y_{lm}(\mathbf{r})$ is one-electron wave function and integration is performed over all angles of \mathbf{k} inside the volume Ω . Equation (1.2.6) enables one to obtain the dispersion relation $E(\mathbf{k})$ of the effective medium. The calculation of the density of the electronic states in the form of equation (1.2.7) can be done using the variation procedure (see Subsection 1.3):

$$\rho(E) = \frac{\delta N(E)}{\delta E} . \quad (2.2.8)$$

The calculations of conductivity are usually performed using Kubo-Greenwood formula [5, 8]:

$$\sigma_E(\omega) = (\pi \Omega / 4\omega) [f(E) - f(E + \hbar\omega)] |D_E|^2 n(E + \hbar\omega) dE , \quad (2.2.9)$$

where ω is a real frequency parameter of Fourier transform for the time-dependent functions, $f(E)$ the Fermi-Dirac distribution function, $D_{E,E'} = \int_{\Omega} \Psi_{E'}^* \nabla \Psi_E d\mathbf{r}$, and $\Psi_{E(\mathbf{k})} = A \exp(i\mathbf{k}\mathbf{r})$ the complex wave vector of the effective medium. The dispersion function $E(\mathbf{k})$ determines the properties of the wave function $\Psi_{E(\mathbf{k})}$ on the isoenergy surface in \mathbf{k} -space. The imaginary part of \mathbf{k} causes damping of the electron wave, due to the absence of long-range structural order. The second possibility for estimating the conductivity comes from the Thouless model [14], where the loss of phase of the electron wave is linked with the structural disorder and is taken into account in a purely phenomenological way through the coherence length λ . The complex wave number $k_R + i(1/2\lambda)$ in this model can now be attributed to the calculated dispersion relation $E(\mathbf{k})$ where R describes the effective radius of scattering sphere. If we calculate the coherence length $\lambda = (1/2)(\text{Im } \mathbf{k})$, then the conductivity can be expressed *via* Fermi level ε_F :

$$\sigma_E(\omega) = (16/3)\pi^2 \lambda n^2(\varepsilon_F) [1 + \omega^2 \lambda^2 / (4\varepsilon_F)] . \quad (2.2.10)$$

Using the dispersion law, the effective mass of electrons can be defined as:

$$m^* = (\partial^2 E / \partial k_R^2)^{-1} . \quad (2.2.11)$$

Thus, the static conductivity can be re-written using Drude formula [15]:

$$\sigma_{E(\mathbf{k})} = \frac{e^2 n^*}{m^*} \tau , \quad (2.2.12)$$

where n^* is the effective electron density, a relaxation time $\tau \approx \frac{l}{v_h}$, $v_h = \left(\frac{3kT}{m^*} \right)^{\frac{1}{2}}$, $l(T)$ the free path.

2.3. Liquid Metal Model

The term “liquid” means the structural disorder of the substance involved, more precisely, only the nearest order is taken into account, as usually considered in the liquid [14-17]. It also means that the distance up to the nearest neighbour (first coordination sphere) maintains whereas the angular coordinates are random. Another condition is that the average density of matter maintains locally also. The term “metal” does not mean the applicability of model only for metals, it was successfully implemented on semiconductors too [6,7]. Thin metal layers as well as nanotubes can be also described in the framework of formalism of a glass-like structure.

To implement this model, we must focus the matter into a single atom (Fig. 6) which will be associated with a crystalline potential in MT -approach, to consider the influence of the nearest vicinity. The neighbour atom

around the studied atom is spread and, in fact, we are working on the one bond distance. The area (2) is a sphere of R_k radius determined from the condition of average matter density preservation. However, to consider the influence of medium we need to “load” the sphere (2) with an effective complex potential, which defines the fading of electromagnetic waves, thereby modelling the disordered medium. The region (3) is under the influence of coherent potential $\Sigma(E)$. After that we must sew the wave functions on the border of regions 2 and 3, superposing the Sovent condition [16], which correspond to the statement that disordered media do not allow the forward scattering.

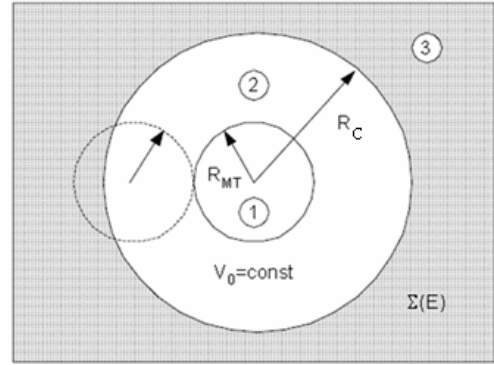


Figure 6. The “liquid” metal model

The spherical symmetry of this system allows us to use partial decomposition techniques and the scattered wave outside the MT-sphere (2), where the potential is constant, can be defined as

$$\psi_l^{(2)} = j_l(kr) - \text{tg } \delta_l n_l(kr). \tag{2.3.1}$$

The next step is to find the dispersion law of the medium (Fig. 7) and the density of states (Fig. 8). In “liquid” model, the argument \mathbf{k} of dispersion function $E(\mathbf{k})$ is a complex: $\mathbf{k}_R + i\mathbf{k}_I$. When using the CPA approach

$$\left(\int_{\Omega_k} \langle \mathbf{k} | \tilde{t} | \mathbf{k}' \rangle d\Omega_k = 0 \right) [4], \text{ this allow us to illustrate the}$$

dispersion law:

The calculation of the density of states (DOS) using the formalism of scattering theory is based on Luttinger theorem [17]. The electron inside a large sphere with the radius R moves in the spherically symmetric potential $V(\mathbf{r})$ decreasing faster than r^{-2} . The scattered partial wave here is:

$$\psi_l(r) = \frac{1}{r} \sin(k'r + \delta_l - \frac{1}{2}l\pi), \tag{2.3.2}$$

approaching to zero at $r \rightarrow \infty$. For wave equation, the Green’s function $G(\mathbf{r}, \mathbf{r}')$ can be used [8]:

$$(\nabla^2 - V(\mathbf{r}) - E)G(\mathbf{r}, \mathbf{r}') = \delta(\mathbf{r} - \mathbf{r}'), \tag{2.3.3}$$

where $G(\mathbf{r}, \mathbf{r}') = \sum_{l,m} Y_{lm}(\mathbf{r})Y_{lm}(\mathbf{r}')G_l(\mathbf{r}, \mathbf{r}')$, $\delta(\mathbf{r} - \mathbf{r}')$ the Dirac’s function and $\int_{\Omega} Y_{lm}(\mathbf{r})Y_{lm}(\mathbf{r}')d\Omega = 1$.

The simplest expression for the DOS through the Green’s function can be written as (see Eq. 2.2.6):

$$\rho(E) = \frac{\delta N(E)}{\delta E} = \frac{2}{\pi} \int \text{Im}\{G(\mathbf{r}, \mathbf{r}', E)\} d\mathbf{r}. \tag{2.3.4}$$

Obviously, the Green’s function should describe the scattered wave outside the MT sphere; on the other hand, it should be the outgoing wave, *i.e.*, satisfied the asymptotic condition in the infinity:

$$G_l(r, r') = cF_l(kr_>)J_l(kr_<), \tag{2.3.5}$$

where $J_l = \cos \delta_l \cdot j_l(kr) - \sin \delta_l \cdot n_l(kr)$, $N_l = -\cos \delta_l \cdot n_l(kr) + \sin \delta_l \cdot j_l(kr)$ [(shifted on phase by 90^0) – similar to small j_l and n_l (Bessel and Neuman functions), $h_l = j_l + in_l$, the using of n_l and h_l are equivalent]

$$F_l = N_l + I_l J_l = [\sin \delta_l \cdot j_l(kr) - \cos \delta_l \cdot n_l(kr)] + I_l [\cos \delta_l \cdot j_l(kr) - \sin \delta_l \cdot n_l(kr)],$$

and then

$$k \frac{N'_L(kR_C) + I_L J'_L(kR_C)}{N_L + I_L J_L} = K \frac{h'_l(KR)}{h_l(KR)}, \tag{2.3.6}$$

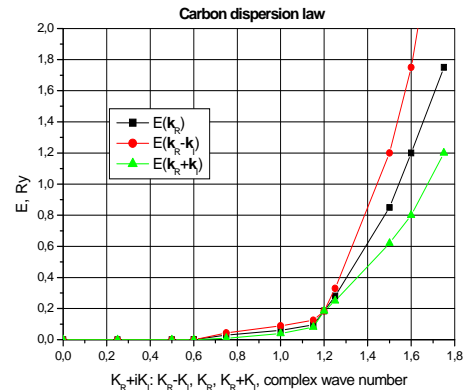


Figure 7. Dispersion of C in “liquid metal model”

where $h_l^+(kr) \propto \frac{\exp(ikr)}{kr}$ – is the modified Hankel function $h_l^+(kr) = n_l - ij_l$, R_C the cluster radius, K – is the complex wave number of effective medium, $k = \sqrt{E}$ – the wave number within the cluster.

After the integration of (2.3.4) by angular and radial coordinates using approximation of “one-atom” cluster in the effective medium with radius R_C (Fig. 5) and the right normalization for the Green’s function, the density function of the electronic states can be written as:

$$\rho(E) = \frac{2}{\pi} \sum_{l=0}^{\infty} (2l+1) \left(\frac{d\delta_l}{dE} - R_C^2 \sqrt{E} [j_l(kR_C) - tg \delta_l n_l(kR_C)]^2 \frac{\partial \gamma_l(E, R_C)}{\partial E} \text{Im} I_l \right) \quad (2.3.7)$$

where

$$\gamma(E, R_C) = k \frac{\cos \delta_l j_l'(kR_C) - \sin \delta_l n_l'(kR_C)}{\cos \delta_l j_l(kR_C) - \sin \delta_l n_l(kR_C)} \text{ is the logarithmic derivatives on the cluster boundary.}$$

The dispersion law looks as follows:

$$\frac{1}{K} \sum_l (2l+1) \exp(i\delta_l(E, K)) \sin \delta_l(E, K) = 0 \quad (2.3.8)$$

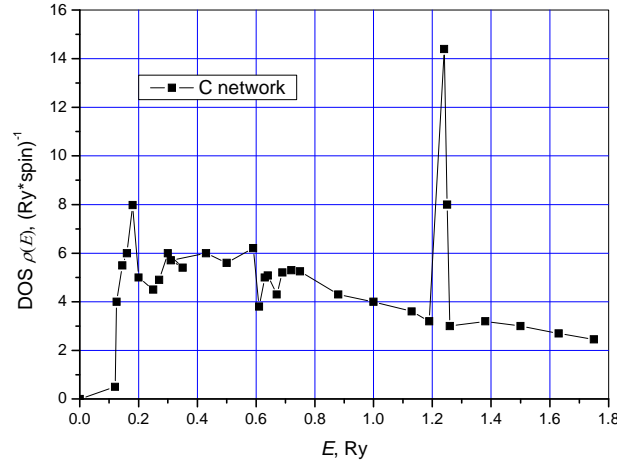


Figure 8. The DOS for carbon in ‘liquid metal model’ (CPA calculations)

Note: If we use ‘liquid metal model’, the atomic configurations do not significant, for we consider only 1 averaged ‘neighbour’ around a basic atom, which is placed in cluster centrum, the zero level is $E_{MTZ} = -2/R_{MT}$, where $R_{MT} = d/2$, d – is the characteristic interatomic distance. No sense also to speak about chirality in the framework of this model, ‘spin’ means 2- double degeneration on spin (+1/2, -1/2)

Another promising application for the *MT*-approach using the “liquid metal model” is the possibility to estimate the specific resistance ρ in the framework of the Ziman’s model [9].

The basic definition is the modified Drude formula for conductivity:

$$\sigma = \frac{1}{\rho} = \frac{ne^2\tau}{m^*}, \quad (2.3.9)$$

where the τ is the effective time free movement, m^* is the effective mass.

If the atoms of liquid metal (or amorphous metal film) are dispersing centres, their distribution is not completely random (while the amplitude of scattering from two atoms located one from another on a distance, circumscribed by a radius-vector \mathbf{R} , is equal: $[1 + \exp(i\mathbf{q}\mathbf{R})]f(\theta)$, where $\mathbf{q} = \mathbf{k} - \mathbf{k}'$, and taking into account multiple scattering:

$$\frac{1}{\sigma} = \rho = \frac{3\pi}{\hbar^2 e^2 v_F \Omega} \int_0^{2k_F} \frac{|V(q)|^2 S(q) q^3 dq}{4k_F^4} \quad (2.3.10)$$

where $\frac{1}{\tau} = N_C v_f \int_0^\pi I(\theta)(1 - \cos \theta) 2\pi \sin \theta d\theta$, $I(\theta) = |f(\theta)|^2$, $f(\theta) = \left(\frac{m}{2\pi\hbar^2}\right) \int V(\mathbf{r}) \exp(i\mathbf{q}\mathbf{r}) d\mathbf{r}$, – the scattering amplitude function $S(\mathbf{q}) = \frac{1}{N_C} \int (1 + \exp(i\mathbf{q}\mathbf{R})) g(\mathbf{R}) d\mathbf{R}$ – the structural factor $V(\mathbf{q}) = \frac{1}{\Omega} \int V(\mathbf{r}) \exp(i\mathbf{q}\mathbf{r}) d\mathbf{r}$ – the Fourier image of potential-scatterer, $L = v_f \tau$, v_f is the Fermi velocity, τ – is the free path time, N_C is the number of scattering centres within the volume Ω , θ is the scattering angle, $\mathbf{q} = \mathbf{k} - \mathbf{k}'$, \mathbf{k} , \mathbf{k}' – are the wave vector before and after a scattering, $g(\mathbf{R})$ – is the pair correlation function of atomic distribution.

2.4. Application of theory for the Ni-CNT contact

A liquid metal model for CNT-Ni interconnect is based on calculation of the mixed dispersion law (Figs. 9, 10):

$$E_{C-Ni}(\mathbf{k}_R) = xE_C(\mathbf{k}_R) + (1-x) E_{Ni}(\mathbf{k}_R). \quad (2.4.1)$$

This model is very sensitive to *ab initio* parameters such as *MT*-radius, cluster radius, potential configurations, etc, which evidently must be optimised.

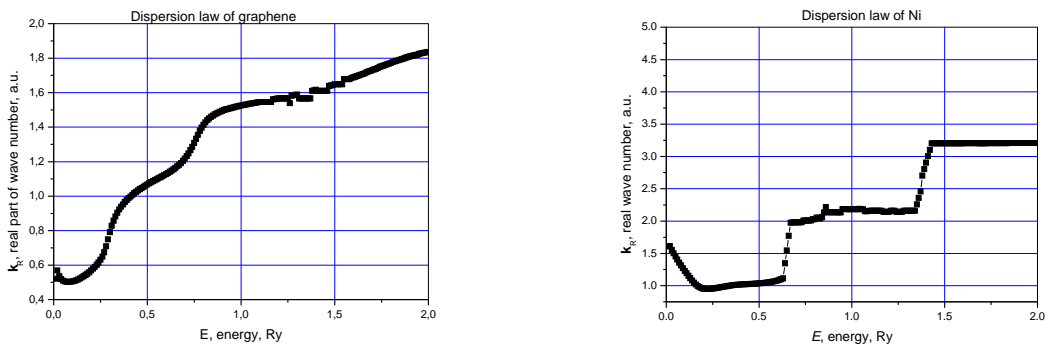


Figure 9. Model dispersion laws

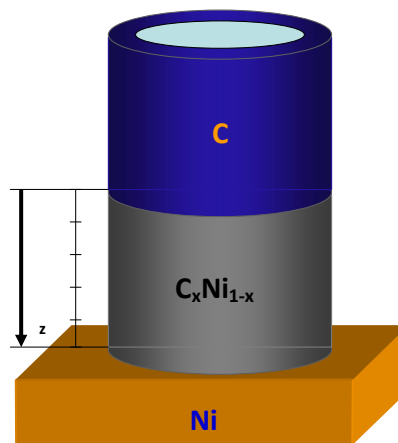


Figure 10. Model of Ni/CNT interconnect

The metal alloy model is used for evaluation of mixed effective mass $m^*_{C-Ni}(E)$, Eq. (2.2.11), which allows us to evaluate both conductivity and resistance in alloy layer. Dependence of effective masses and specific resistance on x are presented in Fig. 11 and Table 1. Taking into account the spectral dependence of the effective mass $m^*(E)$ and estimating the spectral resistivity $\rho_x(E)$, we should estimate the average layer resistivity ρ_x as follows:

$$\rho_x = \frac{\int_0^{E_{fin}} \rho_x(E) dE}{E_{fin}}, \quad (2.4.2)$$

where E_{fin} is the evaluation of conduction band wideness. The stoichiometry coefficient $x(z)$, where z is the ring layer coordinate.

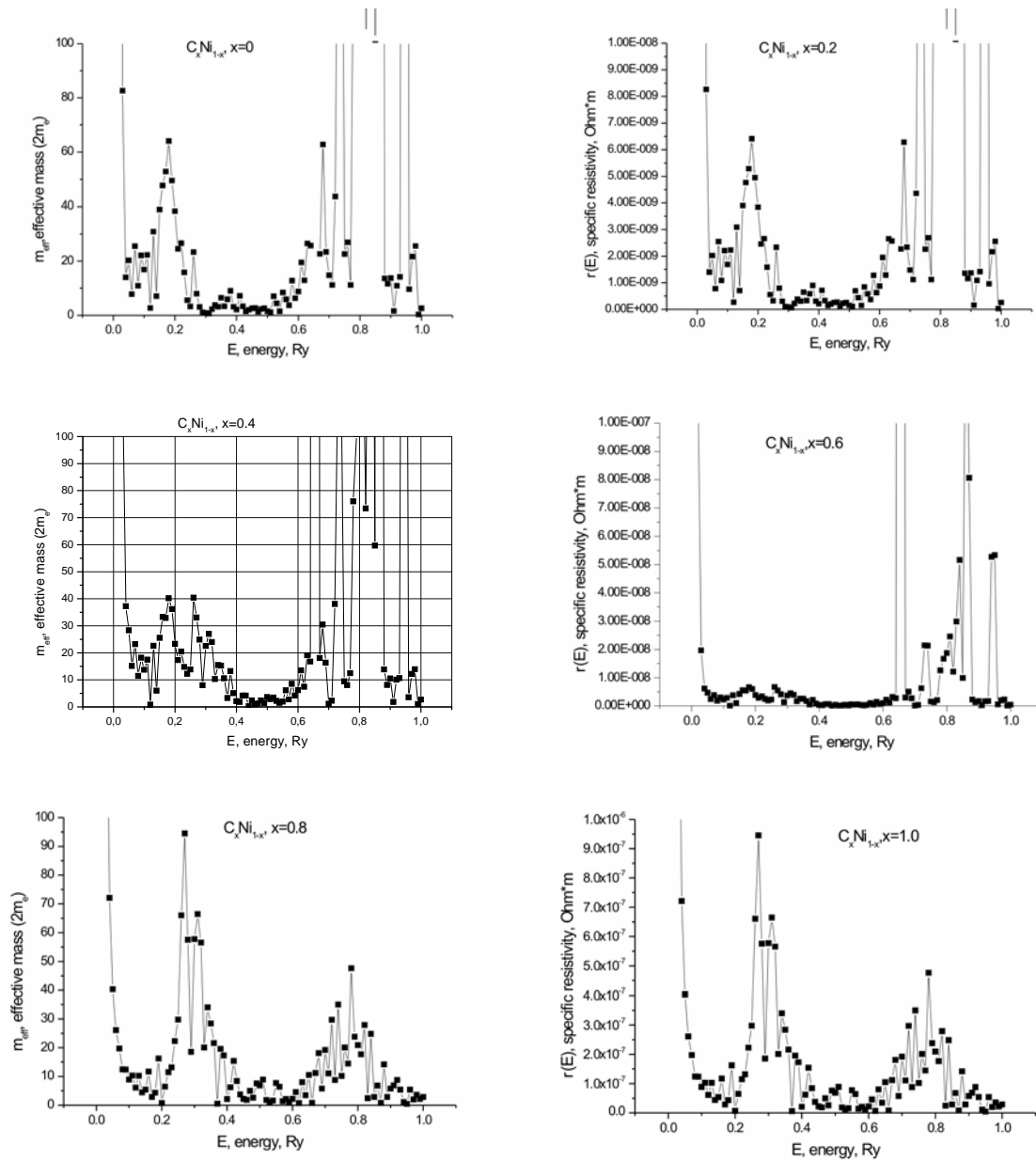


Figure 11. Effective masses and specific resistivities C_xNi_{1-x}

Table 1. Dependence of specific resistivity ρ on alloy composition (x)

No.	x	Layer resistivity C_xNi_{1-x} , $\rho(x)$, $Ohm \cdot nm$
1	0.00	0.80724504E+02
2	0.10	0.81333489E+02
3	0.20	0.82188841E+02
4	0.30	0.83330555E+02
5	0.40	0.84871658E+02
6	0.50	0.87061935E+02
7	0.60	0.90460375E+02
8	0.70	0.96249458E+02
9	0.80	0.10819738E+03
10	0.90	0.14581056E+03
11	1.00	0.82312308E+04

The integral resistivity of the contact C-Ni ring imaged in Fig. 10 can be obtained by integration:

$$R = \int_0^{l_0} \rho(x(z)) \frac{dz}{S} = \frac{1}{\pi(r_2^2 - r_1^2)} \int_0^{l_0} \rho(x(z)) dz, \quad (2.4.3)$$

where S is the nanotube cross-section, r_1 and r_2 are radii of internal and external walls of CNT. If $z = c_0 x$ is proposed as linear, where c_0 is the scaling coefficient, we can rewrite Eq. (2.4.3) as:

$$R = \int_0^1 \rho(x(z)) \frac{dz}{S} = \frac{k_0}{\pi(k_2^2 R_2^2 - k_1^2 R_1^2)} \int_0^1 \rho(x) dx, \quad (2.4.4)$$

which can be applied for any geometry of tube on the basement of calculated resistance unit.

Resistance of C-Ni contact = 0.10643274E+04 Ohm, where $R_1 = 0.10000E-08$ m, $R_2 = 0.20000E-08$ m – are the internal and external radii of conventional nanotube, $k_1 = 1, k_2 = 1, k_0 = 20nm$ – are the scaling coefficients, $\int_0^1 \rho(x) dx = 0.50154819E+03$ Ohm·nm – is the integral resistivity of a contact area,

$$w = \frac{k_0}{\pi(k_2^2 R_2^2 - k_1^2 R_1^2)} = 0.21220841E+10 \text{ m}^{-1}, \quad k_0 = 0.20000000E-07 \text{ m}, \quad S = 0.94246974E-17 \text{ m}^2.$$

Example of resistance recalculation:

1) The contact diffusion length: $k_{0,new} = 50$ nm, $r_1 = 50$ nm, $r_2 = 100$ nm, $k_{1,new} = 50, k_{2,new} = 50,$

$$\frac{k_{0,new}}{\pi(k_{2,new}^2 R_2^2 - k_{1,new}^2 R_1^2)} = w_{new} \cdot \text{Recalculation coefficient: } \frac{w_{new}}{w} = \frac{50^2}{\frac{20}{1^2}} = 10^{-3},$$

Thus, the new resistance: $R_{new} = 0.10643274E+04 * 10^{-3}$ Ohm = 1.064 Ohm

2) The contact diffusion length: $k_{0,new} = 20$ nm, $r_1 = 50$ nm, $r_2 = 100$ nm, $k_{1,new} = 1, k_{2,new} = 0.75,$

$$\frac{w_{new}}{w} = \frac{\frac{20}{1^2(2^2-1)}}{\frac{2,25-1}{20}} = \frac{3}{1,25} = 2,4 \quad \text{Thus, } R = 0.255438576 \text{ E+04 Ohm.}$$

Conclusions

The model of liquid metal alloy model is a convenient calculation scheme which is based on the simplest atomic configuration. But the multiple scattering theory and cluster approach leads to reasonable results. At the same time, there are some essential parameters of calculation, which may demand the optimisation procedure. These parameters are $R_{MT}, R_C, E_{fin}, r_1, r_2, k_0, E_{fin}$. In particular the dispersion law and electronic density of states calculations are very sensitive from R_{MT}, R_C . At the same time the geometry (r_1, r_2, k_0) and conduction band wideness, Fermi velocity, the length of free way, structure factor etc which define the kinetics of electronic transport must be carefully analysed. The temperature dependence of a contact resistance must be investigated also on the basement of kinetics electron gas. The dependence of integral resistance on structural modifications in C_xN_{1-x} contact can be taking into account in the framework of poly-atomic cluster model, using the same multiple scattering conception and effective medium approach (namely, CPA-coherent potential approximation.

References

1. Tans, S.J., Verschueren, R.M., and Dekker, C. Room-temperature transistor based on a single carbon nanotube, *Nature*, Vol. 393, 1998, pp. 49-52.
2. Martel, R., Schmidt, T., Shea, H.R., and Avouris, Ph. Single- and multi-wall carbon nanotube field-effect transistors, *Appl. Phys. Lett.*, Vol. 73, 1998, pp. 2447–2449.
3. Tersoff, J. Contact resistance of carbon nanotubes, *Appl. Phys. Lett.*, Vol. 74, 1999, pp. 2122–2124.
4. Shunin, Yu.N. and Budilov, K. Electronic structure and resistivity of copper, *Comput. Model. New Technol.*, Vol. 5(1), 2001, pp. 42-84.

5. Shunin, Yu.N. and Schwartz, K.K. Correlation between electronic structure and atomic configurations in disordered solids. In: *Computer Modelling of Electronic and Atomic Processes in Solids* / Eds. R.C. Tennyson and A.E. Kiv. Dordrecht/Boston/London: Kluwer Ac. Publ., 1997, pp. 241-257.
6. Shunin, Yu.N. and Schwartz, K.K. Calculation of the electronic structure in disordered semiconductors, *Phys. stat. solid (b)*, Vol. 135, 1986, pp. 15-35.
7. Shunin, Yu.N. and Schwartz, K.K. Electronic structure and conductivity of disordered semiconductors, *Tech. Phys.*, Vol. 39, 1994, pp. 1025-1031.
8. Economou, E.L. *Green's Functions in Quantum Physics. 3rd Ed., Solid State Ser., Vol.7.* Berlin/Heidelberg: Springer Verlag, 2006. 477 p.
9. Ziman, J.M. *Models of Disorder.* New York, London: Cambridge University Press, 1979. 600 p.
10. Dovesi, R., Saunders, V.R., Roetti, C., Orlando, R., Zicovich-Wilson, C.M., Pascale, F., Civalleri, B., Doll, K., Harrison, N.M., Bush, I.J., D'Arco, Ph., and Llunell, M. *CRYSTAL-06 User Manual.* University of Turin, 2006.
11. Zhukovskii, Yu.F., Popov, A.I., Balasubramanian, C., and Bellucci, S. Structural and electronic properties of single-walled AlN nanotubes of different chiralities and sizes, *J. Phys.: Cond. Matt.* , Vol. 18, 2006. S2045-S2054.
12. Zhukovskii, Yu.F., Pugno, N., Popov, A.I., Balasubramanian, C., and Bellucci, C. Influence of *F* centers on structural and electronic properties of AlN single-walled nanotubes, *J. Phys.: Cond. Matt.* , Vol. 19, 2007. 395021 (1-18)
13. Zhukovskii, Yu.F., Jacobs, P.W.M., and Causá, M. On the mechanism of the interaction between oxygen and close-packed single-crystal aluminum surfaces, *J. Phys. Chem. Solids*, Vol. 64, 2003, pp. 1317-1331.
14. Thouless, D.J. *The Quantum Mechanics of Many-body Systems.* New York: Acad. Press, 1961. 175 p.
15. Smith, N.V. Drude theory and the optical properties of liquid mercury, *Phys. Lett. A*, Vol. 26, 1968, pp. 126-127.
16. Soven, P. Coherent potential model of substitutional disordered alloy. *Phys. Rev.*, Vol. 156, 1967, pp. 809-813.
17. Luttinger, J.M. and Ward, J.C. Ground-state energy of a many-fermions system. *Phys. Rev.*, Vol. 118, 1960, pp. 1417-1427.